

Bi-tellurides in gold veins, BiTel Knoll (CLY prospect), southeastern British Columbia, Canada

Nigel J. COOK, Natural History Museum, University of Oslo, Boks 1172 Blindern, NO-0318 Oslo, Norway

Cristiana L. CIOBANU, Mineralogy Group, South Australian Museum, North Terrace, Adelaide, S.A. 5000 Australia and Department of Earth and Environmental Sciences, University of Adelaide, S.A., 5005, Australia

William R. HOWARD, 215 Silver Mead Cres. NW Calgary AB T3B 3W4, Canada

Abstract. Gold ores from BiTel Knoll (CLY Group), Nelson District, B.C., Canada, contain a number of Bi minerals, notably tellurides and tellurosulphides of Bi. The Bi-mineral assemblage is varied from sample to sample. Typical minerals are joséite-B ($\text{Bi}_4\text{Te}_2\text{S}$), joséite-A ($\text{Bi}_4\text{S}_2\text{Te}$), unnamed Bi_2Te , hedleyite (Bi_7Te_3), ingodite ($\text{Bi}(\text{Te},\text{S})$), native bismuth (Bi), bismuthinite (Bi_2S_3) and ikonolite (Bi_4S_3). The Bi-assemblages in the two veins are of reduced type (species with $\text{Bi}/(\text{Te}+\text{S}) \geq 1$). They differ in the presence of native bismuth only in the Blue Quartz vein and ingodite only in the Eloise vein. Native gold is present as inclusions in Bi-mineral patches in both veins. Gold concentrations measured in Bi-minerals from the Eloise vein are in the range between 0.02 and 57 ppm. Concentrations vary by orders of magnitude between samples in different locations. Phase relationships and the distribution of Au in Bi-minerals support a hypothesis in which the mineralization, although formed from Au-Bi-Te-S melts exsolved from fluids, has been overprinted by a subsequent (orogenic?) event.

Key Words: gold ores, veins, tellurides, bismuthinite, electron probe data, laser ablation, ICP mass spectra, British Columbia, Canada

1. INTRODUCTION

The CLY Group of claims comprises a set of veins and skarns located near the contact to the mid-Cretaceous Bunker Hill sill, an outlier of the Wallack Creek granite, which in turn belongs to the Bayonne magmatic belt. This marks the boundary between Lower Jurassic rocks of the Quesnel Terrane to the NW and Paleozoic sedimentary rocks of the Kootenay Terrane. The geological setting of the region, structural geology of the claim area, and sulphide mineralogy have been described by Howard (this volume).

Some of the veins are sulphide-poor (at BiTel Knoll in the NE part of the claims area), others are sulphide (pyrite-pyrrhotite) rich (Bunker Hill) or are veins overprinting earlier skarn (Lefevre). All the veins contain variable amounts of gold. Geochemistry shows a strong correlation between Au and Bi in all veins in the claims area (Howard, this volume). This is most pronounced in the veins from the BiTel Knoll area, where higher gold assays are expressed as visible gold and, in some

cases, are accompanied by bismuth minerals, including tellurides and tellurosulphides (collectively called ‘tellurides’ here). Other veins, in Bunker Hill, are characterised by micron-sized inclusions of gold within pyrite (pseudomorphosed after pyrrhotite). Rare Bi-minerals were, however, identified, but appear restricted to sulphosalts such as cosalite.

This study focuses on two veins from BiTel Knoll (Eloise vein and Blue Quartz vein) in which both native gold and bismuth minerals are present. Hand specimens from the veins show a pronounced fracturing. The blue colour is considered to be due to incorporation of bismuth minerals within the quartz. Polished blocks prepared from other veins (e.g., Ella and Clarissa veins) contained μm -sized inclusions of native gold within quartz but did not contain Bi-minerals.

The aim is to present the mineral associations in these veins. We also carried out LA-ICP-MS analysis on the Bi-minerals in the Eloise vein sample to determine their gold contents. Such

measurements are useful, together with paragenetic observations, to discuss the distribution and partitioning of gold in different species and comment on their genesis.

2. SAMPLE DESCRIPTION

Blue quartz vein

The only sulphide in the samples is scarce molybdenite, both in host rock and vein. Iron- and Ti-oxides are abundant in the host rock (biotite schist/amphibolite?), whereas rare-earth minerals are present only in the vein. Both bismuth minerals and gold (~Au₇₅Ag₂₅) occur as µm-sized blebs along the fractures in quartz (Fig. 1). The Bi-mineral assemblage is dominated by joséite-A (Bi₄S₂Te), bismuthinite and native bismuth. Other species are joséite-B (Bi₄Te₂S), hedleyite (Bi₇Te₃) and ikunolite (Bi₄S₃). The blebs can be mono-component, but are typically multi-component, in which native gold is also part of the assemblage (e.g., Fig. 1a). Joséite-B is found especially in blebs that contain native bismuth (Fig. 1b) and also Bi₂Te and/or hedleyite (Fig. 1a, c). Sulphur-rich blebs dominated by joséite-A may occasionally also contain ikunolite (Fig. 1d). These Bi-rich associations are similar to those typically reported from gold skarns. Although the samples are affected by weathering, native

bismuth is part of the primary association, based on mutual relationships with the Bi-tellurides (e.g., Fig. 1b, c). Most abundant are blebs containing an association of native Bi + bismuthinite.

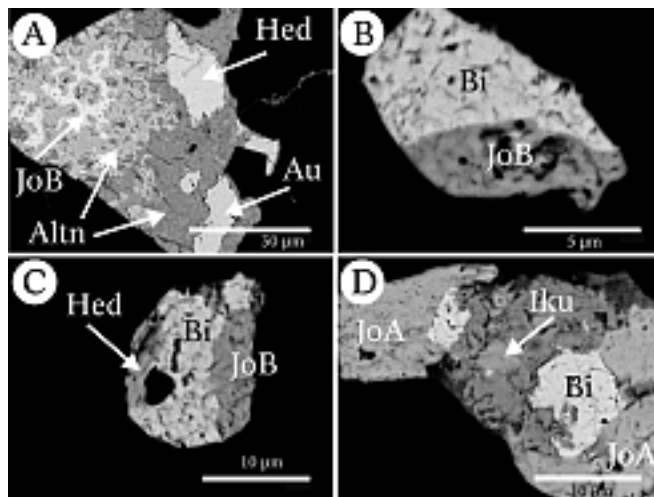


Figure 1. Back-scattered electron images showing assemblage of gold and Bi-minerals (Blue Quartz vein). Altn: alteration, Au: gold, Bi: native bismuth, Hed: hedleyite, Iku: ikunolite, JoA: joséite-A, JoB: joséite-B.

Eloise vein

Polished blocks from samples at two locations along the vein were studied. In both locations, native gold and Bi-minerals are present, although they differ in association.

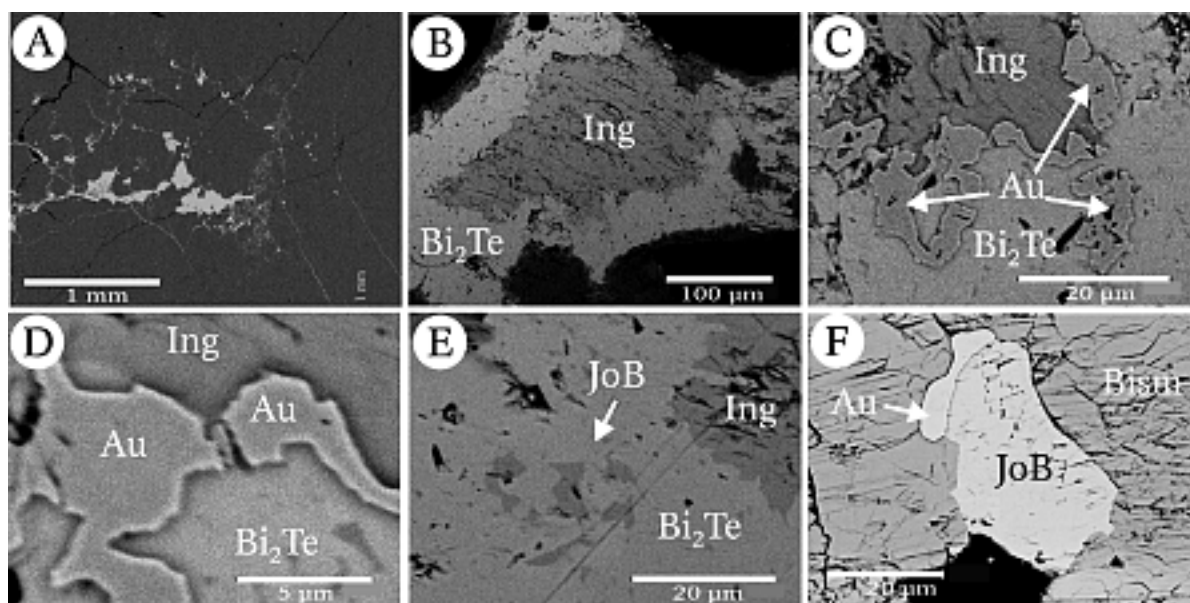


Figure 2. Back-scattered electron images showing Bi-minerals in sample 'Eloise' (a-e) and 0412a (second location, f). Bi₂Te: unnamed Bi₂Te, Bism: bismuthinite, Ing: ingodite, JoB: joséite-B, Au: gold.

In one of the two, several relatively coarse (50-100 µm) patches of Bi-minerals (<50% remain non-weathered) occur in the vein as larger masses interconnected by a fine network of filled fractures (Fig. 2a, bright). The patches consist mainly of (i) ingodite, Bi(Te,S), and unnamed Bi₂Te (Fig. 2b, c) and (ii) ingodite and coarse symplectites of joséite-A and joséite-B. Bismuthinite may be part of the assemblages. Native gold is present in (i) as a rim at the contact between the two Bi-minerals (Fig. 2c, d). It also forms separate grains, tens of µm in size, at the margins of assemblage (i), connected by veinlets to the Bi-mineral mass. Ingodite is enveloped by unnamed Bi₂Te. The latter contains irregular µm-sized inclusions of joséite-B (Fig. 2e).

Samples from the second location, on the northern side of the vein, contain mm-sized patches of bismuthinite (<50% remain non-weathered). Tellurides, such as ingodite, joséite-A and joséite-B occur either as 10-20 µm-sized inclusions, or as larger (100-500 µm) masses at the margin of bismuthinite. The inclusions can be euhedral or are slightly deformed. A comparable deformation is observed along the cleavage planes of host bismuthinite. Scarce native gold is present as <10 µm-sized inclusions in bismuthinite, sometimes combined with tellurides (Fig. 2f). The same coarse symplectites between joséite-A and -B as in samples from the other location described above are observed in the larger patches at the margins of bismuthinite.

3. ELECTRON MICROPROBE DATA

A CAMECA SX-51 instrument at Adelaide Microscopy, Adelaide, South Australia was used, at an operating voltage of 20 kV and beam current of 20 a.

Microprobe data for identified species are presented in Tables 1-3. Data for unnamed Bi₂Te and hedleyite in the Blue Quartz Vein were obtained by EDAX and are not included in the table. We point to the variable contents of Pb in joséite-A and -B and that Pb is preferentially enriched in joséite-A in the Eloise vein. In the

Blue Quartz vein, neither joséite-A nor -B contain Pb, which is actually higher in the coexisting ikunolite.

Table 1. Mean analyses of Bi-minerals in the sample '0414'.

	Jo-A	Jo-B	Iku	Bism
	n=13	n=2	n=2	n=3
Cu	0.00	0.00	0.00	0.06
Pb	0.17	0.06	4.15	0.10
Cd	0.22	0.17	0.26	0.17
Bi	80.00	74.15	83.66	80.16
Sb	0.11	0.13	0.02	0.15
Te	11.97	21.84	0.97	0.04
Se	0.12	0.06	0.15	0.02
S	6.36	2.98	10.33	18.52
Total	99.09	99.37	99.56	99.53

Empirical formulae:

Joséite-A: (Bi_{3.95}Pb_{0.02}Sb_{0.01})_{3.98}Te_{0.97}S_{2.05}Se_{0.02}

Joséite-B: (Bi_{4.00}Sb_{0.01})_{4.01}Te_{1.93}S_{1.05}Se_{0.01}

Ikunolite: (Bi_{3.72}Pb_{0.19})_{3.91}S_{3.09}

Bismuthinite: (Pb_{0.01}Cu_{0.01}Bi_{1.97})_{1.99}S_{3.01}

Table 2. Mean analyses of Bi-minerals in the 'Eloise' sample.

	Jo-A	Jo-B	Ing	Bi ₂ Te	Bism
	n=8	n=6	n=10	n=12	representative
Cu	0.00	0.00	0.00	0.00	0.23
Pb	3.03	0.68	1.74	0.79	1.03
Cd	0.32	0.27	0.18	0.25	0.04
Bi	75.34	74.99	68.54	76.78	78.73
Sb	0.11	0.17	0.15	0.32	0.46
Te	14.39	21.49	23.54	22.09	0.02
Se	0.10	0.11	0.15	0.21	0.17
S	6.29	2.88	5.57	0.34	18.31
Total	100.59	99.58	99.87	100.77	98.99

Empirical formulae:

Joséite-A: (Bi_{3.68}Pb_{0.15}Sb_{0.01})_{3.84}Te_{1.15}S_{2.00}Se_{0.01}

Joséite-B: (Bi_{4.03}Pb_{0.04}Sb_{0.02})_{4.08}Te_{1.89}S_{1.01}Se_{0.02}

Ingodite: (Bi_{0.94}Pb_{0.02})_{0.97}Te_{0.53}S_{0.50}Se_{0.01}

Unnamed Bi₂Te: (Bi_{1.97}Pb_{0.02}Sb_{0.01})_{2.00}(Te_{0.93}S_{0.06}Se_{0.01})_{1.00}

Bismuthinite: Cu_{0.03}Cu_{0.02}Bi_{1.96}S_{2.98}Se_{0.01}

Table 3. Mean analyses of Bi-minerals in the sample '0412'.

	Jo-A	Jo-B	Ing	Bism
	n=9	n=7	n=16	representative
Cu	0.00	0.00	0.00	0.34
Pb	2.89	0.42	3.29	0.73
Cd	0.20	0.27	0.30	0.00
Bi	75.57	74.13	66.96	79.04
Sb	0.11	0.14	0.16	0.41
Te	13.99	21.09	21.65	0.11
Se	0.10	0.07	0.06	0.03
S	6.31	3.24	5.81	18.83
Total	99.17	99.37	98.24	99.53

Empirical formulae:

Joséite-A: (Bi_{3.70}Pb_{0.14}Sb_{0.01})_{3.85}Te_{1.12}S_{2.01}Se_{0.01}

Joséite-B: (Bi_{3.97}Pb_{0.02}Sb_{0.01})_{4.01}Te_{1.85}S_{1.13}Se_{0.01}

Ingodite: (Bi_{0.93}Pb_{0.05})_{0.98}Te_{0.49}S_{0.53}

Bismuthinite: (Pb_{0.02}Cu_{0.03}Bi_{1.95}Sb_{0.02})_{2.02}S_{2.98}

4. LA-ICP-MS ANALYSIS

Analysis was carried out on the material from Eloise only. The small size of the phases in the Blue Quartz vein precluded satisfactory analysis.

Experimental

LA-ICP-MS analysis was carried out using the Agilent HP4500 Quadripole ICP-MS instrument at CODES, University of Tasmania, equipped with a high-performance New Wave UP-213 Nd:YAG Q-switched laser ablation system and MEOLaser 213 software operating at 5 Hz. We performed spot analyses (12-80 μm in diameter, depending on size of the target mineral), monitoring the following isotopic abundances: ^{197}Au , ^{130}Te , ^{209}Bi , ^{208}Pb , ^{107}Ag , ^{77}Se , ^{121}Sb , ^{57}Fe , ^{65}Cu , ^{66}Zn and ^{75}As . Total analysis time was 90s (30s pre-ablation and 60s ablation time). Calibration was performed on a doped pyrite standard; Bi served as the internal standard for the tellurides and bismuthinite. Detection limits for gold were 0.01 to 0.05 ppm.

Results

In the 'Eloise' sample, we analysed (1) Symplectites of joséite-A and -B, (2) ingodite and (3) unnamed Bi_2Te (Figs. 3 and 4, with Au concentrations given in ppm). Au concentrations in the Bi-tellurides ranged from <1 ppm to 57 ppm. Representative LA-ICP-MS depth profiles are shown in Figs. 5 and 6. In the first patch (Fig. 3), three LA-ICP-MS spot analyses of Bi_2Te give Au contents stretching across an order of magnitude (3.6 to 57 ppm). We note the excellent correlation between the Au signal and the Ag and As signals on Fig. 5. Antimony, Pb and Se show trends parallel to Bi and Te, at values in agreement with microprobe data. Although steady for the first third of the ablation, the Au signal jumps over one order of magnitude and is then steady again for the remainder of the spot.

In the second patch (Fig. 4), the maximum gold value was obtained from a symplectite of joséite-A and -B (26 ppm). Two LA-ICP-MS spot analyses of coexisting ingodite give 3 and 10 ppm. These

values are two orders of magnitude higher than in the first patch (0.05 ppm). The profile (Fig. 6) was integrated for Au over the second half of the ablation where Sb increases and Pb decreases. Gold is below detection limits in the first half of the profile. As in the previous case, the Au signal is paralleled by the As and Fe signals.

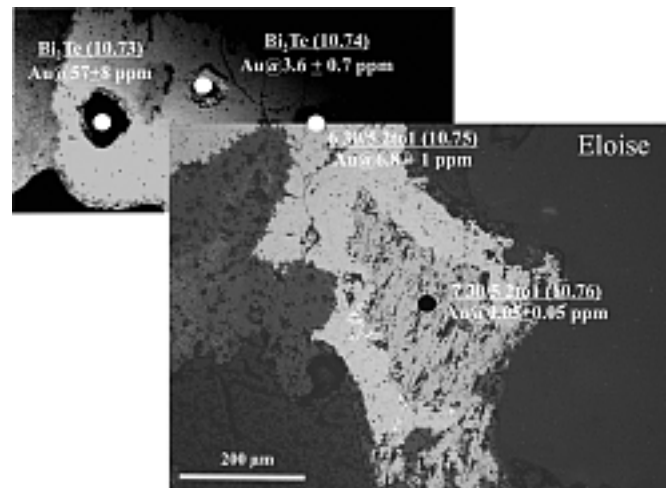


Figure 3. Back-scattered electron images showing ablated grains of Bi-tellurides in sample 'Eloise'. Gold concentrations are given in ppm.

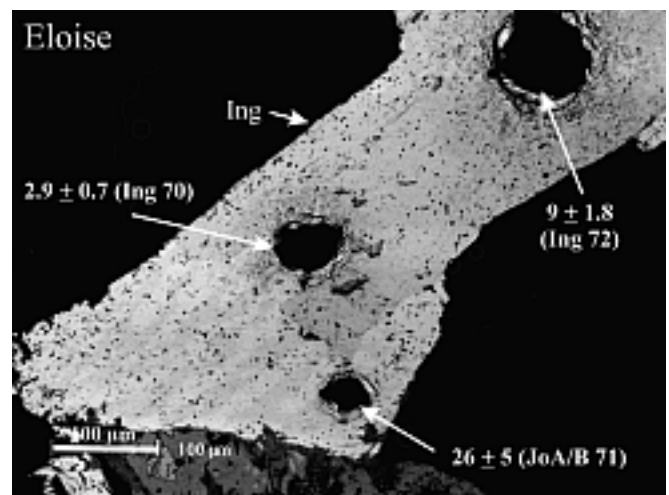


Figure 4. Back-scattered electron images showing ablated grains in sample 'Eloise'. Gold concentrations are given in ppm.

In samples from the second location, two analyses were made of the joséite-A and -B symplectites in the same area (Figs. 7 and 8), with values of 0.13 and 0.65 ppm. Ingodite was analysed by four spots of which two gave Au values below the detection limit (ca. 0.005 ppm);

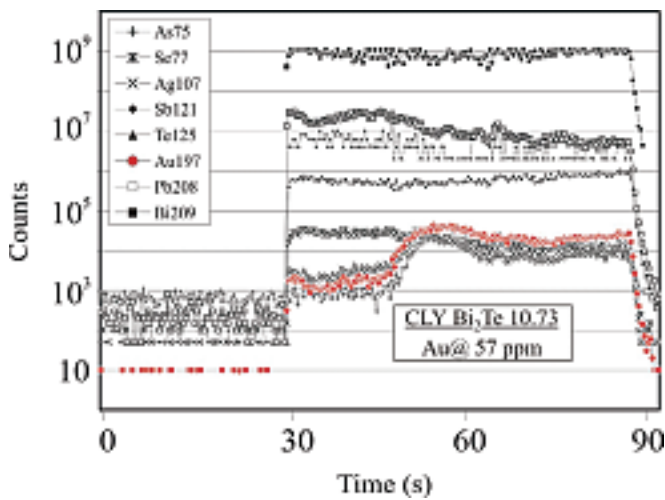


Figure 5. Laser ablation profile of a representative grain of Bi_2Te (point 73, see figure 3). Note that Au concentrations are strongly correlated with Ag and As.

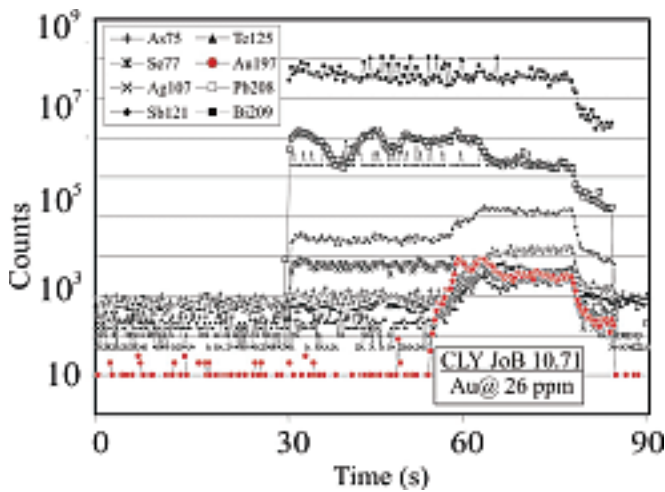


Figure 6. Laser ablation profile of a symplectite between joséite-A and -B (point 71, see figure 4). Note that the first half of the spectra after activation of the laser (30-55s) shows no Au (or Ag) present. Following transition into an included mineral at ca. 55s, Au, Ag and Sb increase markedly.

patch as the tellurides (Fig. 7) and an additional five spots were taken from another patch in which tellurides form small inclusions (attempts to determine Au in one of these inclusions failed because the laser intersected a gold inclusion below the surface). Gold values stretch over two orders of magnitude: 0.02 to 2 ppm in the first case, and from 0.07 to 0.42 ppm in the second.

Figure 9 shows the 11 individual spot analyses of bismuthinite, arranged in order of increasing Au content. Gold contents correlate well with those of Ag, as well as both As and Fe. The other minor

components in bismuthinite (Pb, Cu, Sb and Se) show generally flat, parallel trends across the dataset. The same correlation between Au and some trace elements (Ag, As, Fe) was noted in individual spot analyses of tellurides above.

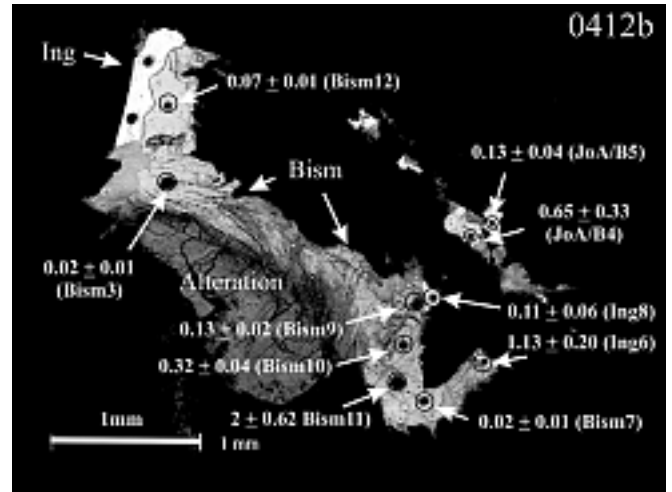


Figure 7. Back-scattered electron images showing ablated grains in sample '0412b'. Au concentrations are in ppm.

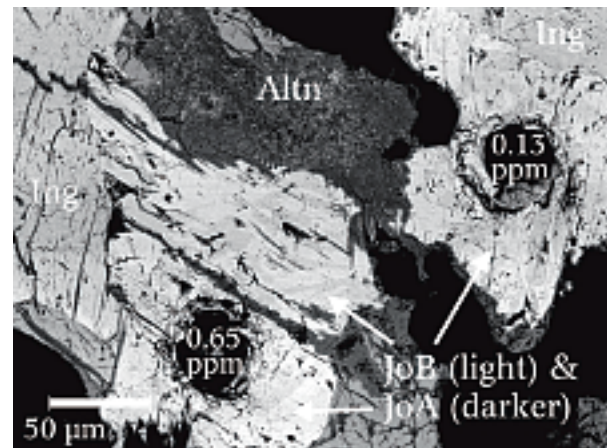


Figure 8. Coarse intergrowths of joséite-A and -B (brighter areas) in bismuthinite matrix (middle grey). LA-ICP-MS laser spots are clearly visible. Scale bar: 50 μm .

The full dataset for tellurides and sulphosalts is summarised in Fig. 10, arranged in order of increasing Au concentration. The figure also shows error bars for each individual analysis. From this, we see that Au contents from the first location are higher by at least one order of magnitude. The gold content in bismuthinite is comparable to that in the coexisting tellurides. The highest Au concentrations do not appear to be restricted to one telluride species in particular. For example, ingodite can be the most and least Au-enriched within individual patches.

ingodite can be the most and least Au-enriched within individual patches.

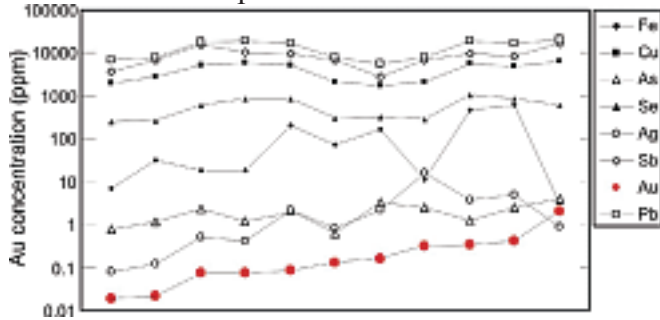


Figure 9. Laser ablation data for individual bismuthinite analyses arranged in order of increasing Au content from left to right. Note that both Ag and Fe correlate with Au. Lead, Cu, Se and Sb (common minor or trace components of bismuthinite) show relatively flat profiles.

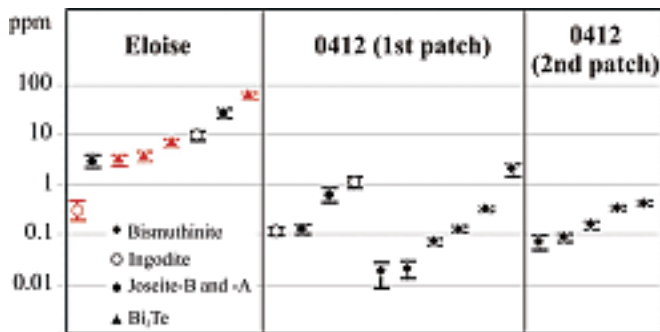


Figure 10. Laser ablation data for individual Bi-telluride analyses arranged in order of increasing Au content, subdivided by sample. For Eloise, values from patch in Fig. 3 are in red and from Fig. 4 in black.

5. DISCUSSION AND CONCLUSIONS

In both veins, native gold is included within Bi-mineral associations that are characteristic for the Bi-rich side of the system Bi-Te-(S). They represent reduced associations (pyrrhotite, magnetite stability) since all species can be at equilibrium with native bismuth given their $\text{Bi}/(\text{Te}+\text{S}) \geq 1$ ratio. Native bismuth is however present only in the Blue Quartz vein, forming associations resembling those known from the gold skarn at Hedley. Native bismuth + Bi_2Te / Bi_7Te_3 and $\text{Bi}+\text{Bi}_2\text{S}_3$ correspond to eutectics at 266°C and 270°C in the Bi-Te and Bi-S systems, respectively. This, together with the droplet-like shape, may be taken to presume their precipitation from fluids in a molten state, as considered for

gold skarns (Meinert, 2000) and intrusion-related veins at Pogo, Fort Knox and elsewhere in the Tintina belt, Alaska (McCoy, 2000). However, the Blue Quartz associations differ from these examples in the fact that they lack maldonite or its breakdown products (symplectites of native gold = bismuth). Maldonite is the Au-bearing phase included in the two eutectic associations from the Bi-rich side of the Au-Bi-Te system ($\text{Bi} + \text{Au}_2\text{Bi}$, 241°C and $\text{Bi}_7\text{Te}_3 + \text{Bi} + \text{Au}_2\text{Bi}$, 235°C). Crystallization from melts will always conclude in forming eutectic associations following partial crystallization along the solvus curve (Ciobanu et al., 2005, 2006a, b). This implies that even though the droplets may have initially been precipitated in a molten state, they have suffered internal redistribution of Au (if this was indeed at all included in the melts). Relationships between phases with Bi_4X_3 ($\text{X}=\text{Te},\text{S}$), i.e., joséite-B replaced by joséite-A and/or ikunolite, also suggest that the Bi-mineral assemblages are overprinted during a subsequent event. This is characterised by fluids with an increased content of S relative to Te (higher S/Te ratios in the replacing phases). Potentially, the same event could have redistributed and/or introduced gold.

The Bi-mineral associations in the Eloise vein differ from the above in that they do not contain primary native bismuth, and also include ingodite, a tellurosulphide with $\text{Bi}/(\text{Te}+\text{S}) = 1$, which is not observed in the Blue Quartz vein. Here, the relationships between (i) phases with the same $\text{Bi}/\text{X}=4:3$ ratio (symplectites of joséite-B and -A) and (ii) skeletal inclusions of joséite-B in Bi_2Te indicate immiscibility via exsolution rather than an overprint. The mantling of ingodite by Bi_2Te , however, and the rim of native gold formed at the boundary between the two (Fig. 2c, d) can be interpreted as replacement of ingodite that also may have released Au. This would explain the low values of Au in ingodite from this patch (0.05 ppm) relative to another in which no native gold is observed (9 ppm). The replacement can be paralleled with the transitory reaction $\text{liquid} + \text{BiTe} = \text{Bi}_5\text{Te}_3 + \text{Au}$ at 374°C in the system Au-Bi-Te. The jump over an order of magnitude in the Au signal obtained during ablation of Bi_2Te (Fig. 5) is indicative of formation of sub- μm -scale

Cook et al., this volume) during any overprinting event that would assist solid-state diffusion and/or fluid infiltration. The good correlation with other elements, such as Fe and As, which do not commonly replace the main components in the structure, also supports such an hypothesis. Although the Au signal across the joséite-B/-A symplectites (Fig. 6) shows a similar jump during the ablation interval, this can be interpreted as preferential concentration of Au in the component with lower Pb and higher Sb (joséite-B), rather than nucleation of Au inclusions. This is concurrent with the lack of evidence for overprinting in this particular patch.

Measured gold concentrations in the same bismuth tellurides within patches from samples in the second location from the Eloise vein are two orders of magnitude lower than those from the first location. There is no preferential concentration of Au in any specific telluride species or in bismuthinite (Fig. 10). Moreover, the ranges of Au values are the same in bismuthinite whether it contains inclusions of native gold or not. The good correlation across the dataset between Au and the same elements observed for the tellurides, i.e., Fe, As, Ag, indicates partitioning of Au at comparable values between the tellurides and the sulphosalt.

The residual Au content in Bi-minerals, the exsolution relationships, and also the fact that all Bi-minerals contain residual amounts of Au support the hypothesis that at Eloise, as in the Blue Quartz vein, they may have formed by crystallization of molten Bi-Te-S-(Au) precipitates. In the Eloise vein, however, no eutectic associations are preserved, given the fact that the overprint has modified the Bi/X ratios in the species. The highly variable gold contents in the Bi-tellurides from one location to another along the vein, as well as between patches in the same sample, indicates the impact of the overprinting event that assisted Au redistribution and is beneficial for nucleation of native Au.

The data presented here, however, needs to be supplemented in order to obtain a better, quantitative assessment of the role played by the

overprinting in the BiTel Knoll veins. This study shows nonetheless the ability of Bi-minerals to incorporate Au and also to track overlapping events by subtle changes in their chemistry. An overprint is shown also by the replacement relationships between Fe-Ti-oxides in the same Bi-mineral samples. The presence of molybdenite (also abundant in other deposits from the same region, e.g., Hedley), as well as REE-phosphates, shows the affiliation of the mineralising fluid to a magmatic source, e.g., Bunker Hill Sill. The subsequent event, with an important role in remobilising and concentrating Au from the pre-existing Bi-Te-(S) assemblages in the veins, may be attributed to one or the other tectonic events (Late Cretaceous?) postdating intrusion emplacement in the area.

REFERENCES

- Ciobanu, C.L., Cook, N.J., Pring, A., 2005. Bismuth tellurides as gold scavengers. In: Mao, J.W., Bierlein, F.P. (eds.) *Mineral Deposit Research: Meeting the Global Challenge*, Springer, p. 1383-1386.
- Ciobanu, C.L., Cook, N.J., Damian, F., Damian, G., 2006a. Gold scavenged by bismuth melts: An example from Alpine shear-remobilisates in Highis Massif, Romania. *Mineral. Petrol.* 87, 351-384.
- Ciobanu, C.L., Cook, N.J., Pring, A., Brugger, J., Netting, A., Danushevskiy, L., 2006b, LA-ICP-MS evidence for the role of Bi-minerals in controlling gold distribution in ores. 12th Quadrennial IAGOD Symposium, Moscow, Russia, 21st -24th Aug. 2006. CD-ROM abstract volume.
- Cook, N.J., Ciobanu, C.L., Danushevskiy, L., 2007, this volume. LA-ICP-MS determination of gold in Bi-minerals from deposits in the Fennoscandian Shield.
- Howard, W.R., this volume. Structural setting and geochemical correlations in bismuth (sulfo)telluride-native gold-bearing veins, CLY Group, B.C., Canada: A reduced intrusion-related gold system.
- McCoy, D.T., 2000, Mid-Cretaceous plutonic-related gold deposits of interior Alaska: metallogenesis, characteristics, gold associative mineralogy and geochronology. Ph.D. thesis, University of Alaska at Fairbanks AK. 245 pp.
- Meinert, L.D., 2000, Gold in skarns related to epizonal intrusions. In: 'Gold in 2000', *Reviews in Economic Geology* 13, 347-375.